JOURNAL OF MATERIALS SCIENCE 29 (1994) 3941–3948

On the chemical vapour deposition of Ti_3SiC_2 from $TiCl_4$–$SiCl_4$–CH_4–H_2 gas mixtures

Part II *An experimental approach*

C. RACAULT, F. LANGLAIS, R. NASLAIN
Laboratoire des Composites Thermostructuraux (UMR-47 CNRS-SEP-UB1), Domaine Universitaire, 3 allée de la Boëtie, 33600 Pessac, France

Y. KIHN
Centre d'Elaboration des Matériaux et Etudes Structurales, Laboratoire d'Optique Electronique–UPR 8011 du CNRS, BP 4347 Toulouse Cédex, France

An experimental study of the deposition of Ti_3SiC_2-based ceramics from $TiCl_4$–$SiCl_4$–CH_4–H_2 gaseous precursors is carried out under conditions chosen on the basis of a previous thermodynamic approach, i.e. a temperature of 1100 °C, a total pressure of 17 kPa, various initial compositions and substrates of silicon or carbon. Ti_3SiC_2 is deposited within a narrow composition range and never as a pure phase. A two-step deposition process is observed, in agreement with the thermodynamic calculations. For a silicon substrate, $TiSi_2$ is formed as an intermediate phase from consumption of Si by $TiCl_4$ and then is carburized by CH_4 into Ti_3SiC_2. For a carbon substrate, the first step is the formation of TiC_x either from consumption of carbon by $TiCl_4$ or by reaction between $TiCl_4$ and CH_4 and then TiC_x reacts with the gaseous mixture to give rise to Ti_3SiC_2. In most cases, Ti_3SiC_2 is obtained as small hexagonal plates oriented perpendicular to the substrate surface. These nano- or micro-crystals are usually co-deposited with TiC_x and to a lesser extent SiC, and their size is increased by increasing the dilution of the gaseous mixture in hydrogen.

1. Introduction

As recently reported, Ti_3SiC_2 exhibits promising thermal and mechanical properties, with potential applications as a new soft ceramic material. A good thermal stability (up to about 1600 K) and an oxidation resistance better than that of titanium carbide were observed for Ti_3SiC_2 prepared from the solid state [1] and a plastic behaviour was reported for the phase deposited by chemical vapour deposition (CVD) [2]. CVD, more suitable for the fabrication of ceramic-matrix composites, has been used up to now with $TiCl_4$–$SiCl_4$–CCl_4–H_2 gaseous precursors, high deposition temperatures ($T \geqslant 1473$ K) and highly diluted initial mixtures.

The first CVD study, from Nickl *et al.* [3], gave a deposition ternary diagram at $T = 1473$ K and $P = 10^5$ Pa. The deposits were prepared on graphite and tantalum substrates. The conditions favourable to the deposition of pure Ti_3SiC_2 were very narrow, particularly in terms of CCl_4 initial molar fraction. Co-depositions of Ti_3SiC_2 with TiC, SiC, $TiSi_2$, Ti_5Si_3 or two of these binary compounds were very often reported. More recently, Goto and Hirai [2] reported the CVD preparation of monolithic Ti_3SiC_2 polycrystalline plates at temperatures higher than 1573 K and a total pressure of 40 kPa. These authors reported lattice parameters and a density in accordance with the crystal structure determined by Jeitschko and Novotny [4]. The (1 1 0) planes of the CVD-Ti_3SiC_2 crystals are preferentially oriented parallel to the deposition surface, giving rise to a deposit morphology with small plates perpendicular to the substrate surface. Other CVD preparations of Ti_3SiC_2 have been reported, but in co-deposition with other materials (e.g. with SiC) from CH_3SiCl_3–$TiCl_4$–H_2 gaseous precursors at $T = 1473$ K and $P = 3.3$ kPa [5]. Ti_3SiC_2 is often obtained with a lamellar morphology, either as pure material or mixed with SiC or TiC [3, 5].

The present experimental study investigates the deposition of Ti_3SiC_2-based ceramics in the CVD system $TiCl_4$–$SiCl_4$–CH_4–H_2. It is the continuation of a previous article dealing with thermodynamic calculations of the equilibrium in the same chemical system [6]. The composition and morphology of the deposits were studied and the deposition processes investigated for silicon and carbon substrates, in correlation with the results of the thermodynamic equilibrium.

2. Experimental procedure

The experiments for the deposition of ceramics in the Ti–Si–C system were performed using a CVD

0022–2461

apparatus with a hot-wall reactor working under reduced pressures (Fig. 1).

The initial gaseous mixture contains (i) $TiCl_4$ directly evaporated from a bath maintained at a constant temperature and transported through a heated flow-meter, (ii) $SiCl_4$ whose vapour pressure is high enough to permit a transport at ambient conditions, (iii) CH_4 as carbon source species and (iv) H_2 as reducing species. The various gas flow rates and consequently the composition of the gas phase were controlled by means of mass flow-meters. The deposition chamber, made of silica glass, was heated resistively up to about 1200 °C, the size of the isothermal hot-zone was 50 mm in diameter and 40 mm in length. The gaseous mixture produced by the CVD reactions was condensed in liquid nitrogen traps. A vacuum rotary pump maintained in the reactor a reduced pressure controlled by a mechanical system.

The substrates used for the CVD experiments were silicon wafers previously treated at 1100 °C under flowing hydrogen and cylindrical graphite pellets 5 mm thick and 10 mm in diameter.

The constitution of the deposits was first identified by X-ray diffraction analysis using a Cu X-ray tube. A scanning electron microscope (SEM) was used to observe the surface and cross-section morphologies of the deposits. The microstructure of typical samples was examined in a transmission electron microscope (TEM) (CM 30-ST from Philips) equipped with a spectrometer (from Gatan) for parallel electron energy loss spectroscopy (PEELS). Bright-field observations and selected-area electron diffraction (SAED) experiments were used for a description of the films at a nanometric scale. Deposits on carbon were prepared for TEM analysis by mechanical polishing and ion-thinning. Deposits on silicon were simply removed from the substrate and crushed into powder.

3. Results and discussion

3.1. Deposition on silicon substrates

3.1.1. Experimental results

On the basis of the thermodynamic calculations [6] and preliminary experiments, the temperature and pressure conditions were chosen in order to favour Ti_3SiC_2 deposition, i.e. $T = 1100$ °C and $P = 17$ kPa. The parameters studied were the initial composition of the gaseous precursor, the ternary composition (characterized by the molar fraction x_{CH_4} and the ratio x_{TiCl_4}/x_{SiCl_4} and the dilution ratio $\alpha = x_{H_2}/x_{TiCl_4} + x_{SiCl_4} + x_{CH_4}$). The duration of the deposition was also investigated to contribute to an understanding of the process involved.

In agreement with the thermodynamic results, the explored initial compositions contained rather high $TiCl_4$ molar fractions and rather low CH_4 molar fractions, while the dilution ratio α varied between 17 and 35. For a 4 h experiment, Ti_3SiC_2 (referred to as T1) occurs only within a relatively narrow composition range, as shown in Fig. 2: x_{TiCl_4}/x_{SiCl_4} between 1 and 2 and x_{CH_4} between 10 and 15%. This composition range seems to widen by diluting in H_2 the gaseous precursor. Ti_3SiC_2 is never obtained as a pure phase, but always with $TiSi_2$ and some amounts of titanium and silicon carbide. When the α ratio increases, SiC deposition seems to be favoured while that of TiC is unfavoured. Deposition experiments of various durations were performed for $x_{TiCl_4}/x_{SiCl_4} = 2$, $x_{CH_4} = 10\%$ and $\alpha = 17$ and 35. For the shorter times (lower than 4 h), Ti_5Si_3 and $Ti_5Si_3C_x$ are formed without Ti_3SiC_2 which is obtained only after a longer duration when Ti_5Si_3 and $Ti_5Si_3C_x$ no longer occur. This result suggests that the Ti_3SiC_2 deposition process on a silicon substrate involves several steps.

The morphology and the microstructure of these deposits were examined respectively by SEM and TEM. Fig. 3 shows an SEM image of a cross-section of a sample (4 h experiment) for $x_{TiCl_4}/x_{SiCl_4} = 2$, $x_{CH_4} = 10\%$ and $\alpha = 17$. A very porous zone is observed within the sample, which probably results from consumption of the silicon substrate. The unetched part of silicon is visible with a thickness much lower than the initial one. Above the porous zone a less porous film seems to have grown. This film still includes small pores, as shown in Fig. 3. As a consequence of this morphology the external layer can be easily removed from the substrate, the fracture occurring at the level of the porous zone (mainly $TiSi_2$). The surface morphology of the films, as observed by SEM, depends highly on the dilution ratio (Fig. 4). For $\alpha = 17$, various blocks of about 1 μm are mixed together in any direction, while for $\alpha = 35$, small plates of more than 1 μm in size seem to have grown perpendicular to the substrate.

Parts of the layer removed from the substrate and crushed into powder were also analysed by TEM (bright-field image mode and SAED) combined with PEELS. For $\alpha = 17$, Ti_3SiC_2 was identified as very small grains of 5 to 10 nm in size joined together in blocks of about 50 to 100 nm (Fig. 5). Titanium and silicon carbides were also present, SiC as grains of 0.5 to 1 μm in size and TiC either as stoichiometric 10 nm grains or non-stoichiometric 50–80 nm grains (i.e. TiC_x with $x \simeq 0.65$). For a higher dilution ratio $\alpha = 35$, Ti_3SiC_2 occurs mainly as monocrystalline small plates or needles 0.05 to 1 μm in size, as shown in Figs 6 and 7. The electron microdiffraction pattern for one of these crystals (Fig. 6b) exhibits a spot diagram which permits one to find the reticular distance $d(0\,0\,1) = 1.765$ nm characteristic of the Ti_3SiC_2 crystal structure. Grains of SiC and non-stoichiometric TiC were also identified for these CVD conditions.

3.1.2. Discussion of deposition mechanisms

From both the previous analyses and the corresponding thermodynamic approach [6], the deposition process on silicon substrate is assumed to occur in two main steps: (i) etching of the substrate giving rise to $TiSi_2$ and (ii) formation of Ti_3SiC_2 from $TiSi_2$.

The highly porous layer of $TiSi_2$ is formed by consumption of the silicon substrate according to the equation

$$2Si + TiCl_4 + 2H_2 \rightarrow TiSi_2 + 4HCl \qquad (1)$$

This reaction, whose Gibbs free energy $\Delta G(1400\ K)$

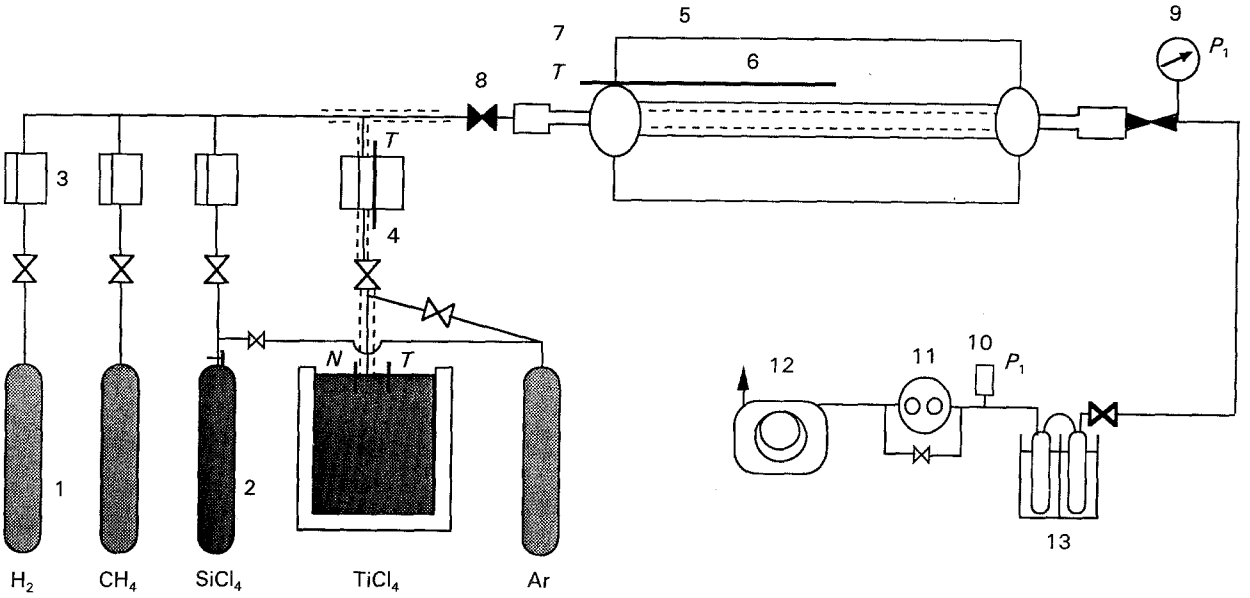

Figure 1 Schematic diagram of the apparatus used for the CVD of Ti_3SiC_2-based ceramics: (1) gaseous precursor, (2) liquid precursor, (3) mass flow-meter, (4) thermostatted line, (5) furnace, (6) reactor tube, (7) thermocouple, (8) shut-off valve, (9) manometer, (10) pressure gauge, (11) pressure controller, (12) vacuum pump, (13) liquid nitrogen traps.

equals 63 kJ mol^{-1}, is favoured by the large excess of hydrogen. This kind of reaction with consumption of the silicon substrate was previously reported to be involved in various related CVD systems such as $TiCl_4$–H_2 and $TiCl_4$–CH_4–H_2 when used to prepare $TiSi_2$ thin films [7–9]. Two dilution ratios can be considered for the purpose of the discussion. For a limited dilution ($\alpha = 17$), the thermodynamic calculations predict the consumption of Si, $TiCl_4$ and H_2 together with the formation of $TiSi_2$, HCl and to a lesser extent gaseous species such as $SiCl_4$, $SiCl_2$, $SiHCl_3$ and $SiCl_3$. Consequently, reactions according to the following equations, with negative Gibbs free energies, are assumed to contribute to the silicon etching:

$$Si + 4HCl \rightarrow SiCl_4 + 2H_2 \quad \Delta G(1400\ K) = -75\ kJ\,mol^{-1} \tag{2}$$

$$Si + 2HCl \rightarrow SiCl_2 + H_2 \quad \Delta G(1400\ K) = -4\ kJ\,mol^{-1} \tag{3}$$

$$Si + 3HCl \rightarrow SiHCl_3 + H_2 \quad \Delta G(1400\ K) = -42\ kJ\,mol^{-1} \tag{4}$$

$$Si + 3HCl \rightarrow SiCl_3 + 3/2H_2 \quad \Delta G(1400\ K) = -29\ kJ\,mol^{-1} \tag{5}$$

For a high dilution ($\alpha = 35$), the consumption of the

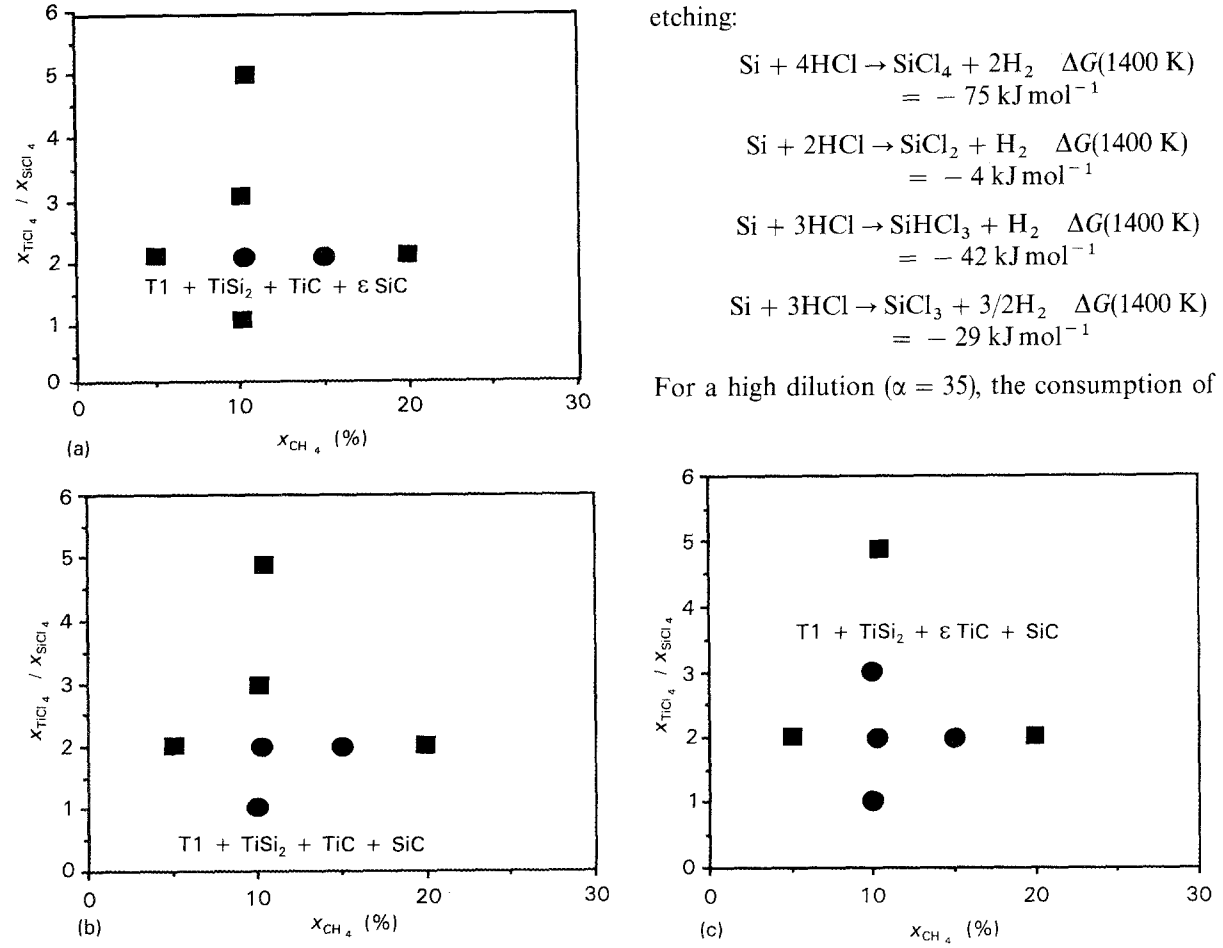

Figure 2 Influence of the composition of the initial gaseous mixtures on the occurrence of Ti_3SiC_2(T1)-based deposits on a silicon substrate for $T = 1100\,°C$ and $P = 17$ kPa: (a) $\alpha = 17$, (b) $\alpha = 25$, (c) $\alpha = 35$. (●) with T1, (■) without T1.

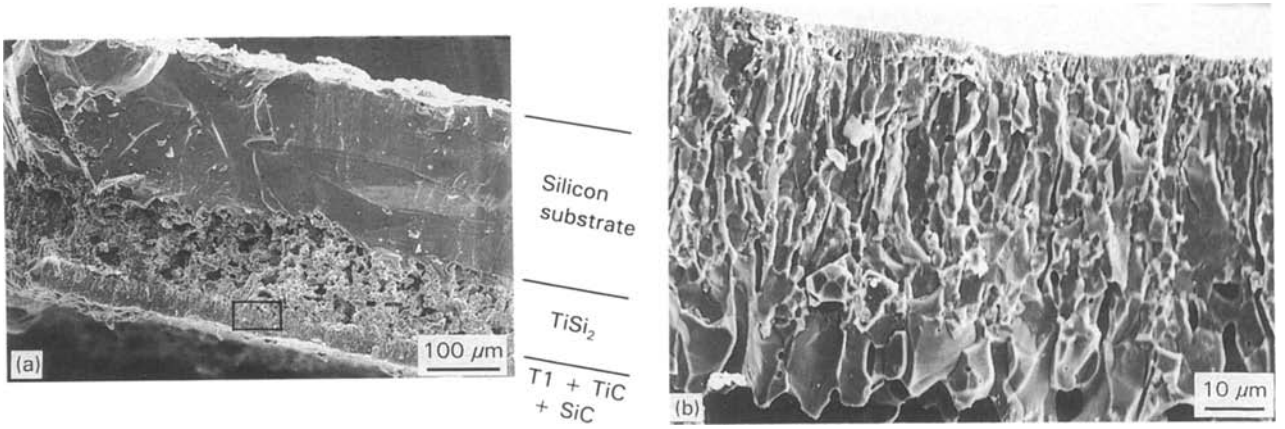

Figure 3 SEM pictures of a cross-section of Ti_3SiC_2-based layers deposited on a silicon substrate for $T = 1100\,°C$, $P = 17\,kPa$, $x_{TiCl_4}/x_{SiCl_4} = 2$, $x_{CH_4} = 10\%$ and $\alpha = 17$.

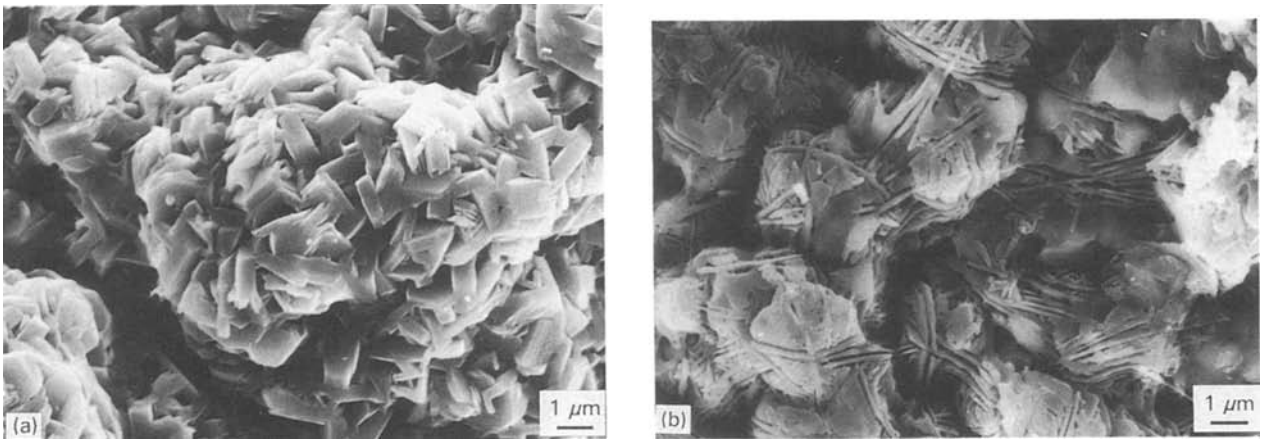

Figure 4 SEM pictures showing the morphological change of the Ti_3SiC_2-based deposit on a silicon substrate for $T = 1100\,°C$, $P = 17\,kPa$, $x_{TiCl_4}/x_{SiCl_4} = 2$, $x_{CH_4} = 10\%$ for various dilution ratios (a) $\alpha = 17$, (b) $\alpha = 35$.

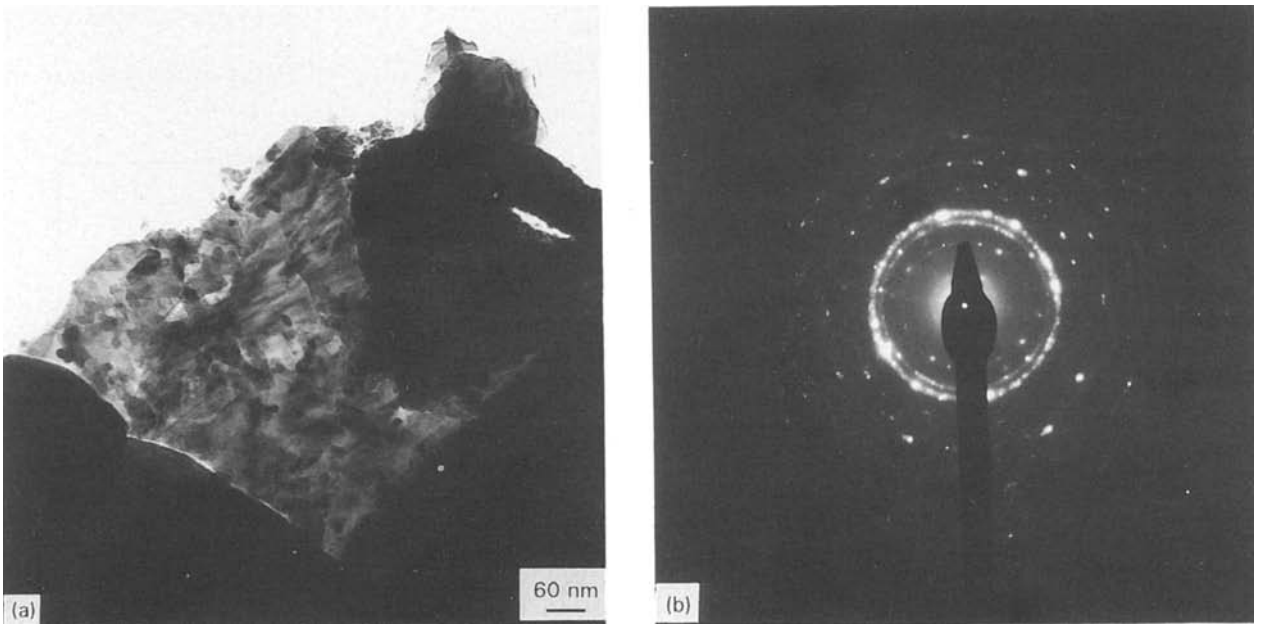

Figure 5 (a) TEM bright-field image of a Ti_3SiC_2-based deposit on a silicon substrate for $T = 1100\,°C$, $P = 17\,kPa$, $x_{TiCl_4}/x_{SiCl_4} = 2$, $x_{CH_4} = 10\%$ and $\alpha = 17$ and (b) SAED pattern of Ti_3SiC_2.

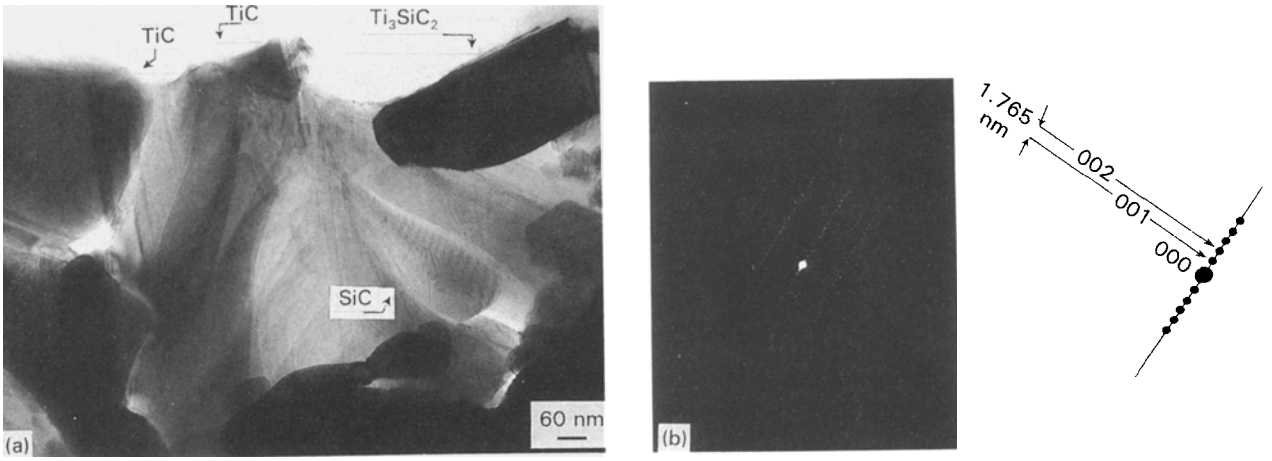

Figure 6 (a) TEM bright-field image of a Ti_3SiC_2-based deposit on a silicon substrate for $T = 1100\,°C$, $P = 17\,kPa$, $x_{TiCl_4}/x_{SiCl_4} = 2$, $x_{CH_4} = 10\%$ and $\alpha = 35$ and (b) the corresponding SAED pattern of Ti_3SiC_2.

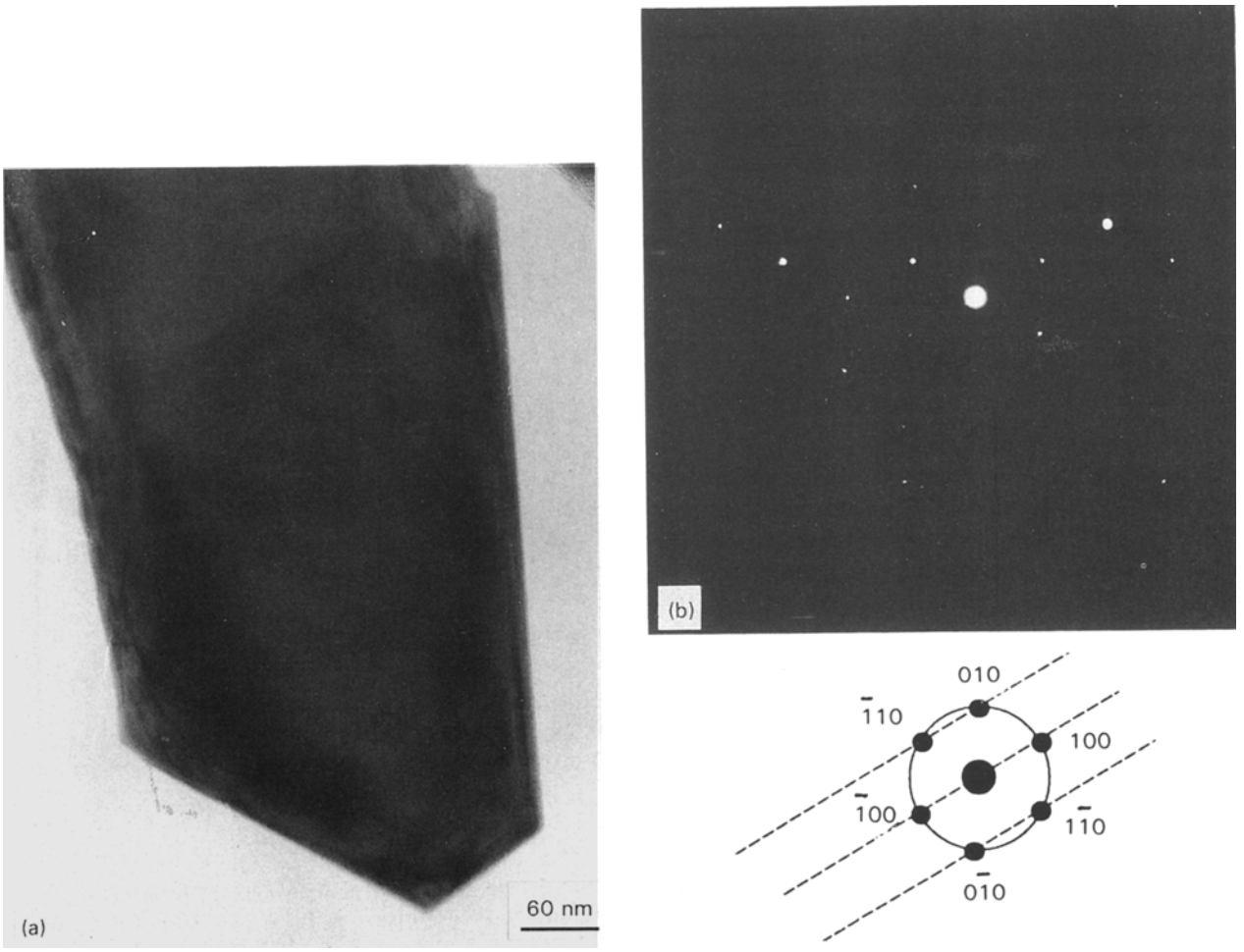

Figure 7 (a) TEM bright-field image of a Ti_3SiC_2 single crystal deposited on a silicon substrate for $T = 1100\,°C$, $P = 17\,kPa$, $x_{TiCl_4}/x_{SiCl_4} = 2$, $x_{CH_4} = 10\%$ and $\alpha = 35$ and (b) the corresponding SAED pattern.

silicon substrate is less important because (i) Equations 2 to 5 are unfavoured by the larger excess of hydrogen and (ii) $SiCl_4$ contributes to $TiSi_2$ formation by reaction with $TiCl_4$, according to the equation

$$TiCl_4 + 2\,SiCl_4 + 6H_2 \rightarrow TiSi_2 + 12\,HCl \quad (6)$$

The second step of the process is the formation of a less porous layer consisting of Ti_3SiC_2 with more or less important amounts of TiC and SiC. The deposition experiments carried out as a function of time have shown that Ti_5Si_3 occurs before Ti_3SiC_2. A carburization of $TiSi_2$ with CH_4 can be assumed according to two successive equations with negative Gibbs free energies:

$$5TiSi_2 + 7CH_4 \rightarrow Ti_5Si_3 + 7SiC + 14H_2$$
$$\Delta G(1400\,K) = -777\,kJ\,mol^{-1} \quad (7)$$

$$Ti_5Si_3 + 6CH_4 \rightarrow Ti_3SiC_2 + 2TiC + 2SiC + 12H_2$$
$$\Delta G(1400\,K) = -665\,kJ\,mol^{-1} \quad (8)$$

These reactions are limited by the excess of hydrogen. Their probable slow rate permits the growth of the various phases Ti_3SiC_2, TiC and SiC. This growth is slower for the highest dilutions (e.g. $\alpha = 35$), which favours particularly the formation of Ti_3SiC_2 single crystals 1 μm in size, as shown in TEM bright-field images (Fig. 6). In contrast, for $\alpha = 17$ most of Ti_3SiC_2 is deposited as nanocrystals. Owing to their reactivity, $TiCl_4$ and $SiCl_4$ are involved simultaneously in homogeneous reactions, as shown by the following equations:

$$TiCl_4 + 1/2H_2 \rightarrow TiCl_3 + HCl \quad \Delta G(1400\,K) = 17\,kJ\,mol^{-1} \tag{9}$$

$$SiCl_4 + H_2 \rightarrow SiCl_2 + 2\,HCl \quad \Delta G(1400\,K) = 71\,kJ\,mol^{-1} \tag{10}$$

$$SiCl_4 + H_2 \rightarrow SiHCl_3 + HCl \quad \Delta G(1400\,K) = 33\,kJ\,mol^{-1} \tag{11}$$

$$SiCl_4 + 1/2\,H_2 \rightarrow SiCl_3 + HCl \quad \Delta G(1400\,K) = 46\,kJ\,mol^{-1} \tag{12}$$

These reactions are favoured by increasing the dilution ratio α.

3.2. Deposition on carbon substrates

3.2.1. Experimental results

The CVD experiments on graphite substrates were carried out under the same conditions as for the silicon substrates, i.e. $T = 1100\,°C$, $P = 17\,kPa$, $\alpha = 17$–35, $t = 4\,h$. The initial composition range favourable to the formation of Ti_3SiC_2 is also limited to rather high $TiCl_4$ molar fractions and rather low CH_4 molar fractions, as indicated in Fig. 8 on the basis of X-ray diffraction analyses. This range is widened by increasing the dilution ratio α, but here again Ti_3SiC_2 is always obtained in co-deposition with titanium carbide and sometimes with SiC, Ti_5Si_3 and/or $TiSi_2$. Experiments carried out for various deposition times have shown that titanium carbide is the first phase formed and Ti_3SiC_2 is obtained only after 2 h. Silicides are co-deposited with Ti_3SiC_2 for the high dilution ratio $\alpha = 35$. On the other hand, on a TiC substrate Ti_3SiC_2 is deposited at the beginning of the experiment without a transient stage.

Unlike the deposits on a silicon substrate, the Ti_3SiC_2-based films are rather adherent when deposited on a carbon substrate. The surface morphology of the films deposited for $x_{TiCl_4}/x_{SiCl_4} = 2$, $x_{CH_4} = 10\%$ and $\alpha = 17$ or 35 is shown in the SEM micrographs of Fig. 9. Hexagonal small plates a few micrometres in size are observed, oriented perpendicular to the substrate surface. The number of these plates is increased by increasing the dilution ratio (Fig. 9b).

The deposits obtained for $\alpha = 17$ were analysed by TEM–PEELS measurements combined with bright-field and electron diffraction experiments have permitted us to identify a non-stoichiometric TiC_x layer (with $x \simeq 0.75$) between the carbon substrate and an upper layer consisting of a TiC–Ti_3SiC_2 mixture.

For an initial composition of the gaseous phase given by $x_{TiCl_4}/x_{SiCl_4} = 1$, $x_{CH_4} = 10\%$ and $\alpha = 35$, the morphology of the deposit was observed by SEM as a function of the experiment duration (Fig. 10). After 2 h, only a few needles occur in a rather dense granular matrix. After 3 h, a significant number of needles seem to have grown from this matrix leaving an important porosity. Finally, after 4 h a lot of needles are formed together with an increasing porosity.

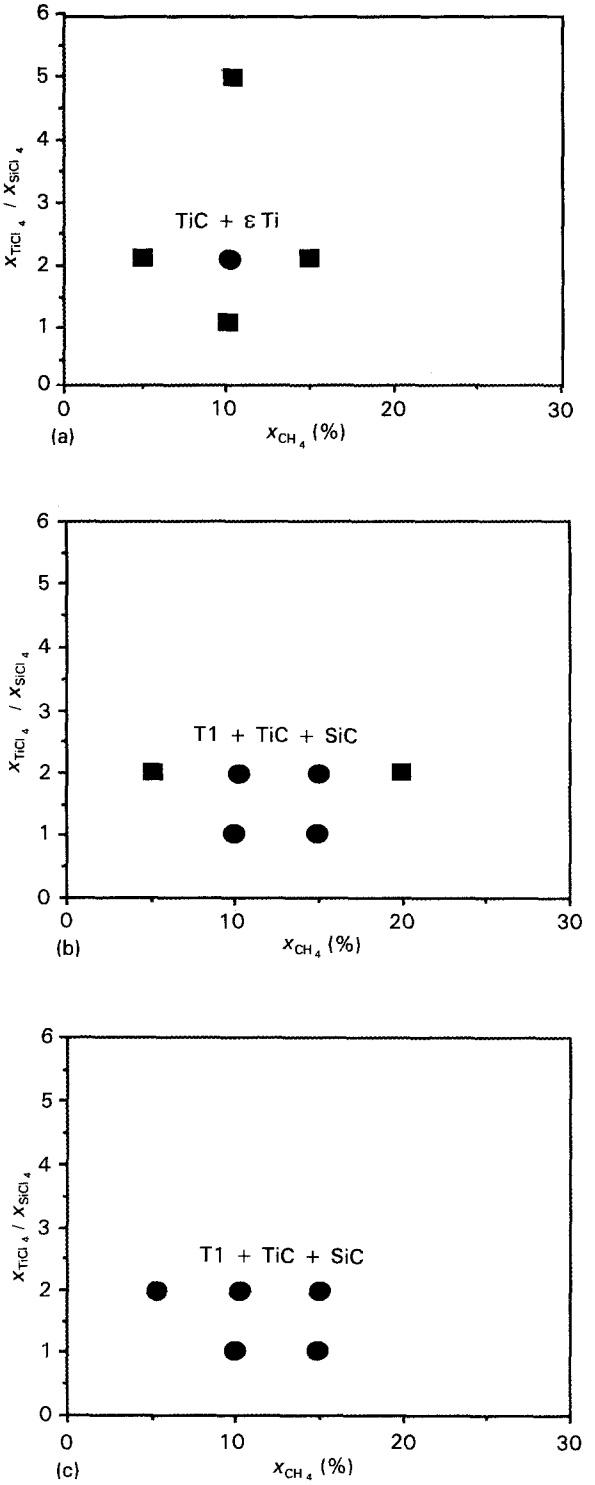

Figure 8 Influence of the composition of the initial gaseous mixtures on the occurrence of Ti_3SiC_2(T1)-based deposits on a carbon substrate for $T = 1100\,°C$, and $P = 17\,kPa$: (a) $\alpha = 17$, (b) $\alpha = 25$, (c) $\alpha = 35$, (●) with T1, (■) without T1.

3.2.2. Discussion of deposition mechanisms

As previously discussed for the silicon substrate, two main steps are assumed to occur in the deposition

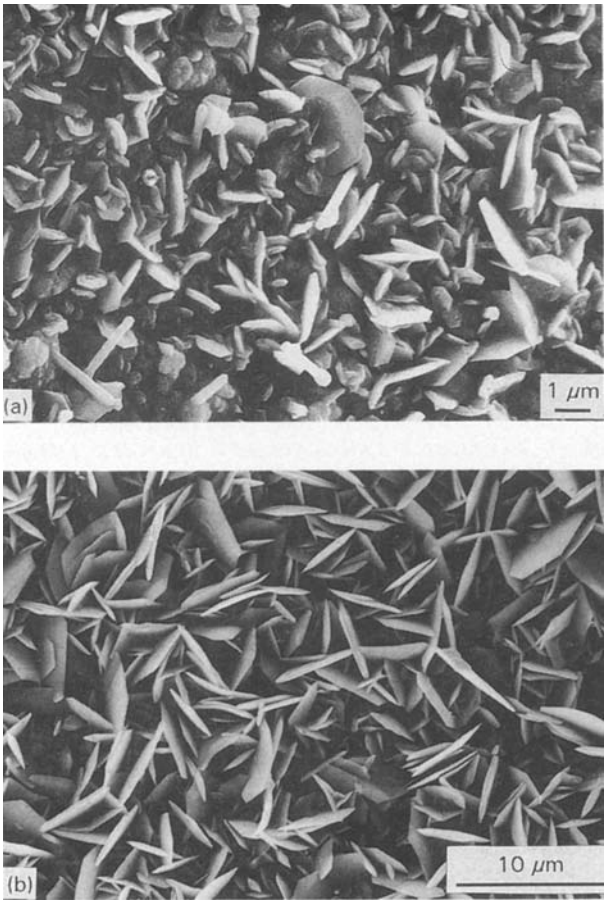

Figure 9 SEM pictures showing the morphological change of the Ti_3SiC_2-based deposit on a carbon substrate for $T = 1100\,°C$, $P = 17\,kPa$, $x_{TiCl_4}/x_{SiCl_4} = 2$, $x_{CH_4} = 10\%$, for various dilution ratios (a) $\alpha = 17$, (b) $\alpha = 35$.

process on a graphite substrate: (i) formation of non-stoichiometric titanium carbide and (ii) reaction of TiC_x with the gaseous mixture to give rise to Ti_3SiC_2.

The thermodynamic calculations for a reactive carbon substrate [6] have predicted (i) the consumption of carbon (less important than that of silicon), $TiCl_4$ and to a lesser extent CH_4 and (ii) the formation of titanium carbide together with small amounts of SiC and $TiCl_3$. On the basis of these theoretical results and the experiments previously reported, the first step involved in the deposition process on a graphite substrate can be represented partly by the equation

$$TiCl_4 + xC + 2\,H_2 \rightarrow TiC_x + 4HCl \qquad \Delta G(1400\,K) = 21\,kJ\,mol^{-1} \qquad (13)$$

This reaction is favoured by the excess of hydrogen and the other species of the initial gaseous mixture can react according to

$$SiCl_4 + CH_4 \rightarrow SiC + 4HCl \qquad \Delta G(1400\,K) = -42\,kJ\,mol^{-1} \qquad (14)$$

Such a titanium carbide formation has been reported for CVD on a carbon substrate in the systems $TiCl_4$–H_2 and $TiCl_4$–CH_4–H_2[10–14]. For high enough temperatures, carbon atoms diffuse from the substrate through the already formed TiC layer and

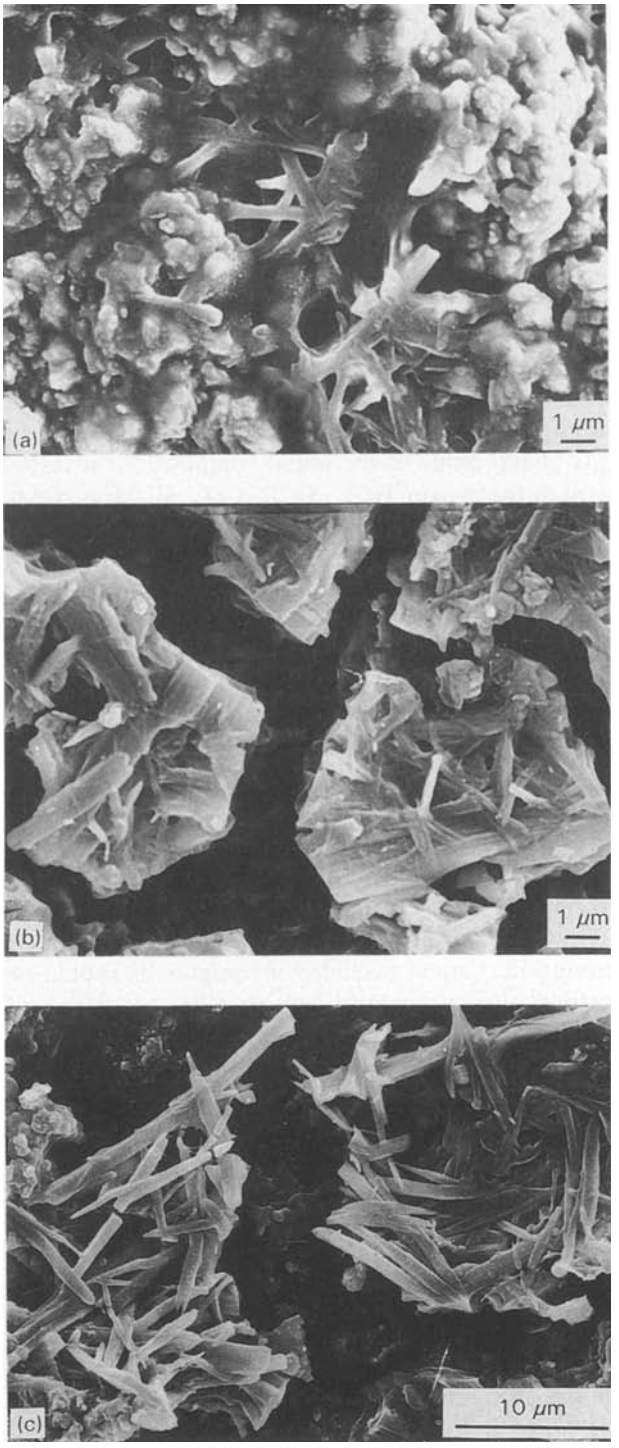

Figure 10 SEM pictures showing the morphological change of the Ti_3SiC_2-based deposit on a carbon substrate for $T = 1100\,°C$, $P = 17\,kPa$, $x_{TiCl_4}/x_{SiCl_4} = 2$, $x_{CH_4} = 10\%$, $\alpha = 35$ and various deposition times (a) $t = 2$ h, (b) $t = 3$ h, (c) $t = 4$ h.

react with the $TiCl_4$–H_2 mixture. Non-stoichiometric titanium carbide can also be formed by reaction between gaseous $TiCl_4$ and CH_4:

$$TiCl_4 + xCH_4 + 2(1-x)H_2 \rightarrow TiC_x + 4HCl \qquad \Delta G(1400\,K) = -17\,kJ\,mol^{-1} \qquad (15)$$

The respective contributions of Reactions 13 and 15 in the process formation of TiC_x cannot be estimated.

A thick enough TiC_x layer seems to be necessary to permit the formation of Ti_3SiC_2. The reaction involved in this second step could be represented by one

of the following equations:

$$TiC_x + 2TiCl_4 + SiCl_4 + (2 - x)CH_4 + 4(1 + x)H_2 \rightarrow Ti_3SiC_2 + 12HCl \quad \Delta G(1400\ K) = 63\ kJ\ mol^{-1} \tag{16}$$

$$3TiC_x + SiCl_4 + 2H_2 \rightarrow Ti_3SiC_2 + 4HCl \quad \text{with } x = 0.67 \quad \Delta G(1400\ K) = 113\ kJ\ mol^{-1} \tag{17}$$

4. Conclusion

The present study emphasizes how difficult is the deposition of the ternary compound Ti_3SiC_2 from the gas phase. None of the initial compositions investigated in the system $TiCl_4$–$SiCl_4$–CH_4–H_2 gives rise to pure Ti_3SiC_2. It is usually co-deposited with titanium carbide whose oxidation resistance is worse than that of Ti_3SiC_2. In addition, the substrates used (particularly the silicon one) are consumed during the first step of the deposition process. Ti_3SiC_2 hexagonal crystals of about 1 μm in size can be obtained if the dilution of the gaseous mixture in hydrogen is high enough. The hexagonal planes seem to grow perpendicularly to the substrate surface, which probably results in thin small plates with a weak cohesion between them.

If some of the results previously reported seem to be unsuitable to specific applications (e.g. the use of Ti_3SiC_2 as an interphase material in ceramic-matrix composites), more extended investigations should be carried out, particularly with (i) other conditions of deposition temperature and pressure, (ii) other gaseous precursors and (iii) other substrates. As far as the substrates are concerned, SiC should be studied because of its comparative thermodynamic stability with respect to the present gaseous precursor [6] and $TiSi_2$ for its ability to give rise more directly to Ti_3SiC_2.

Acknowledgements

The authors wish to thank Société Européenne de Propulsion (SEP) and CNRS for their support via a grant to C. R.

References

1. C. RACAULT, F. LANGLAIS and R. NASLAIN, *J. Mater. Sci.* **29** (1994) 000.
2. T. GOTO and T. HIRAI, *Mater. Res. Bull.* **22** (1987) 1195.
3. J. J. NICKL, K. K. SCHWEITZER and P. LUXENBERG, *J. Less-Common Met.* **26** (1972) 335.
4. W. JEITSCHKO and H. NOWOTNY, *Mh. Chem.* **98** (1967) 329.
5. R. A. LOWDEN, K. L. MORE, T. M. BESMANN and R. D. JAMES, *Mater. Res. Soc. Symp. Proc.*, **168** (1990) 159.
6. C. RACAULT, F. LANGLAIS and C. BERNARD, *J. Mater. Sci.* **29** (1994) 000.
7. A. BOUTEVILLE, A. ROYER, A. BOUAMRANE and J. C. REMY, *Le vide–Les couches minces* **232** (1986) 291.
8. E. MASTROMATTEO, J. L. REGOLINI, C. D'ANTERROCHES, D. DUTARTRE, D. BENSAHEL, J. MERCIER, C. BERNARD and R. MADAR, in Proceedings of 11th International Conference on CVD, 14–18 October 1990, Seattle, edited by K. E. Spear and G. W. Cullen (Electrochemical Society, Pennington, 1990) p. 459.
9. V. ILDEREM and R. REIF, *J. Electrochem. Soc.* **135** (1988) 2590.
10. O. KUBASCHEWSKI, H. VILLA and W. A. DENCH, *Trans. Faraday Soc.* **52** (1956) 214.
11. L. AGGOUR, E. FITZER and J. SCHLICHTING, in Proceedings of 5th International Conference on CVD, 21–26 September 1975, Buckinghamshire, UK, edited by J. M. Blocher, H. E. Hintermann and L. H. Hall, (Electrochemical Society, Princeton, 1975) p. 600.
12. H. E. HINTERMANN and H. G. GASS, in Proceedings of 4th International Conference on CVD, October 1973, Boston, US, edited by G. F. Wakefield and J. M. Blocher, (Electrochemical Society, Princeton, 1973) p. 107.
13. J. N. LINDSTROM and S. AMBERG, *ibid.* p. 124.
14. K. G. STJERNBERG, H. G. GASS and H. E. HINTERMANN, *Thin Solid Films*, **40** (1977) 40.

Received 3 December 1993
and accepted 19 January 1994